



An Empirical Approach for Quick Assessment of Hazard and Safe Height of Steep-Cut Rock Slopes in Garhwal Himalayas

Lal Hruaikima¹ · Mahendra Singh¹ ·
Sarada Prasad Pradhan² · Jaspreet Singh^{2,3}

Received: 13 April 2023 / Accepted: 26 September 2023 / Published online: 25 October 2023
© The Author(s), under exclusive licence to Indian Geotechnical Society 2023

Abstract Accessibility and all-weather functioning of the roads in Himalayas form the backbone of the overall development of the region. All-weather roads are being constructed in the region to cater to the needs of this region and provide quick accessibility to remote areas. Majority of roads are constructed along the hill slopes. Construction of new roads as well as the widening project involves the excavation on hill side of the slope. As a consequence, steep-cut slopes are formed at the side of the road. In principle, adequate analysis and design is warranted while taking up construction activities. However, rigorous slope stability analysis for each section is not always feasible. The field engineers therefore rely on personal experience, judgment and perception, especially when quick decisions are required. Looking at the problem and the importance of hill roads in the Himalayas, urgent need for developing site-specific tools is being felt in organizations dealing with mitigation activities in this region. The tools are required not only at the time of construction but also during the maintenance and emergent situation of natural disasters and also to look

out for safe alternate routes. In the field of rock mechanics, rock mass classification systems have been found to be very effective in addressing similar problems. Rock mass rating (Bieniawski, in: Transaction of the South African Institution of Civil Engineers, 1973), slope mass rating (Romana in: International symposium on the role of rock mechanics in excavations for mining and civil works, International Society of Rock Mechanics, Zacatecas, 1985), geological strength index (Marinos et al. in Bull Eng Geol Environ 64:55–65, 2005. <https://doi.org/10.1007/s10064-004-0270-5>; Morelli in Geotech Geol Eng 35:2803–2816, 2017. <https://doi.org/10.1007/s10706-017-0279-8>; Marinos et al. in: Underground works under special conditions, 2010. <https://doi.org/10.1201/noe0415450287.ch2>) and the Q systems (Barton et al. in Rock Mech 6:189–236, 1974. <https://doi.org/10.1007/BF01239496>) have been used in the past. In the present manuscript, the applicability of the Joint Factor concept (Ramamurthy in Indian Geotech J 8:1–74, 1985; Ramamurthy and Arora in Int J Rock Mech Min Sci 31:9–22, 1994. [https://doi.org/10.1016/0148-9062\(94\)92311-6](https://doi.org/10.1016/0148-9062(94)92311-6); Singh et al. in Rock Mech Rock Eng 35:45–64, 2002. <https://doi.org/10.1007/s006030200008>) is extended to propose an empirical approach for quick assessment of hazard of rock slopes for cut slopes in Garhwal Himalayas. The main objective of the present study is to come out with a methodology to work out an approximate value of the safe height of steep-cut rock slopes. The study has been conducted on steep-cut rock slopes of Garhwal Himalayas. Site investigations followed by desk studies have been done to determine the important parameters of the discontinuities observed in the field. Joint Factor concept is used for evaluating the instability of cut rock slopes. Charts are suggested to assess the hazard and safe height of steep-cut rock slopes based on simple inputs which can be easily obtained in the field. Validation of the proposed approach was done by assessing the stability of

✉ Lal Hruaikima
lalhruaikima@ce.iitr.ac.in
Mahendra Singh
mahendra.singh@ce.iitr.ac.in
Sarada Prasad Pradhan
sppradhan@es.iitr.ac.in
Jaspreet Singh
jassidhu45@gmail.com

- 1 Department of Civil Engineering, IIT Roorkee, Roorkee, Uttarakhand, India
- 2 Department of Earth Sciences, IIT Roorkee, Roorkee, Uttarakhand, India
- 3 Department of Earth Sciences, Simon Fraser University, Burnaby, BC V5A1S6, Canada

cut rock slopes from five different sites. It can be concluded that the observation made in the field and the result obtained from the chart are in agreement with each other.

Keywords Slope stability · Joint Factor · Safe height · Rock mass classification

Introduction

In India, more than 15% of the total land area exceeding 0.49 million sq. km is affected by landslides [10, 11]. Majority of these landslides are in the Himalayan region. Frequent failures along steep-cut rock slopes in these regions cause disruption to transportation facilities and pose massive threat to the social and economic growth of the region. The rocks encountered along hill roads are invariably intersected by geological discontinuities, mainly the joints. Complex geology, adverse climatic conditions, anthropogenic activities and cutting of side slopes are considered to be the leading cause behind the large number of slides [12, 13]. The removal of toe support due to the cutting of slopes results in an imbalance in the equilibrium of rock, which may lead to the failure of the slope. The landslide issue becomes more severe if a slope failure occurs on a transportation corridor which is lifeline of the region or near townships. During the last few years, the widening of roads in the Indian Himalayas has been taken up in a big way, especially in the Garhwal region [14, 15]. The widening is done by cutting the rock on the side slope to some height. Increased incidents of slope instability and road blockage are being experienced at many places indicating unsafe rock cut height at the section. The agencies involved in mitigating activities need tools and techniques for quick hazard assessment and safe height of the cut slopes based on simple and easy-to-obtain inputs from the field. In practice, kinematic analysis followed by limit equilibrium analysis or numerical analysis is done to assess the instability of the rock slopes. In addition, some empirical methods are also adopted. Several rock mass classification systems have been used worldwide to assess the instability of rock masses (RMR, SMR, GSI, Q -slope) [13, 16–30].

In Indian context, some recent notable contributions with regard to rock slope stability issues have been done by adopting the rating systems. This includes the slope mass rating (SMR) [21, 31–33], the rock mass rating [16, 32–34], the geological strength index [16, 34], the rockfall hazard rating system [31, 35–37] and the Q slope system [13, 30, 38].

Rocks in the Himalayan region are invariably jointed, fractured, weathered and exhibit a high degree of variability in their engineering response. [12, 39–41] Extensive geological and geotechnical investigations are required to assess the safe cut height of the rock slopes. Though comprehensive

investigations are generally done during the execution of road widening projects, it is not feasible to extensively investigate each and every section. Also, there has been an alarming increase in the occurrence of extreme events like cloud bursts and flash floods during the last few decades. These events give rise to emergent situations, and quick decisions are required for planning alternate routes or to repair the exiting routes. In addition to the inherent parameters of the rock slope, if a rough assessment of the safe height of the cut rock slope could be made with reasonable accuracy, the strategies for mitigating landslide hazards can be formulated successfully.

The present article proposes an approach using which a rough estimate of safe height of cut rock slope can be made by using easy-to-obtain parameters in the field. The approach is derived by correlating the safe height with strength of the rock mass. Joint Factor concept, an indigenously developed classification system, is used in the present study and a novel index J_{f_slope} is defined to quantify the instability of a rock slope. Charts are presented to assess the hazard due to the step-cut rock slope. These charts are presented based on the data collected from steep-cut rock slopes in Garhwal region of the Himalayas. In its present form, the approach is site specific and needs further studies for extending it to other regions.

Background

The part of National Highway-58 (NH-58), which connects towns of Rishikesh and Badrinath in India, continuously experiences deterioration due to the ongoing road widening projects. Being the lifeline of this region and also having strategic importance, the route observes heavy traffic around the year, which further shoots up significantly during summers due to extensive tourism and religious activities [21, 31, 32, 42]. The up-hill side of the roads generally comprises of cut rock slope. The rocks invariably comprise of discontinuities; joints being the most common form of discontinuity. Joint characteristics, namely, dip, dip direction of joint with respect to the slope direction, frequency and surface characteristics of the joint planes have significant influence in governing the strength of the rock mass of the cut slope. As a consequence, the safe cut height of the rock slope is predominantly influenced by joint characteristics. Some attempts have been made in the past to assess the hazard due to rock slopes by considering the joint characteristics [17, 22, 43, 44]. Generally, these attempts are based on classification approaches [13, 17, 20, 22, 23, 25, 26, 28, 29, 45–47].

In the present study, the safe height of an almost vertical rock slope is correlated with the strength of the rock mass. The presence of joints makes the rock mass weaker and anisotropic in strength behavior and hence induces instability.

To get an insight into stability at a rock slope, an adequate understanding of the influence of joint characteristics on the strength of the rock mass is a must. Joint Factor concept [8, 9, 48–50] has been an important contribution, which helps in quantifying the influence of rock joints on the strength of the rock mass. The concept was developed based on extensive laboratory tests on natural and jointed rocks having strength varying from 5 MPa to a maximum of 120 MPa [7]. The concept was initially aimed to assess the strength and deformational behavior of jointed rocks. It was concluded that the strength of a rock mass is substantially influenced by the angle between the joint plane with respect to the loading direction, frequency and surface roughness of the joints. To quantify the effect of joint attributes collectively, a weakness coefficient, Joint Factor, was introduced [8, 9, 49, 50].

During the initial phases of the development of the Joint Factor concept, laboratory tests were performed on small specimens having single or multiple joints. Later the applicability of the concept was extended to specimens of rock mass comprising large number of elemental blocks [9, 50]. Specimens of jointed rock mass were prepared by piling elemental blocks in various fashions in order to achieve different dips of joints and interlocking conditions. The specimens were tested under uniaxial loading conditions. Figure 1 shows photographs of typical failed specimens [50]. Depending on the orientation of joints and the interlocking conditions, the specimens were found to fail in splitting, shearing, rotation and sliding. Interestingly, the failure modes observed in this study (Fig. 1) have striking similarities with the failure modes of rock slopes observed in the field. Rock slopes in

Fig. 1 Different modes of failure **a** splitting **b** shearing **c** rotational **d** sliding. (After Singh [50])



fields generally fail due to planar failure, wedge failure, toppling and circular failure.

It was found that the strength of jointed rock mass is closely related with Joint Factor (J_f) and failure mode (Fig. 1 after Singh [50] and Singh et al. [9]). Resemblance in failure modes observed in laboratory study indicates the great potential of the basic concept of Joint Factor to investigate rock slope instability problems. Keeping this in mind, a comprehensive field study was performed in which 50 steep-cut rock slopes were investigated. Several field visits were made. Data comprising of slope geometry, field mapping of joints, rock strength and observed instability was collected. Applicability of Joint Factor concept was examined, and a modification was made to make it applicable to steep cut rock slopes. Finally, charts were produced to assess the hazards due to rock slopes.

Study Area

For the current study, 50 rock slopes along the highway from Rishikesh to Kaudiyala were selected for analysis (Fig. 2). Geologically, the study area comprises of various meta-sedimentary rocks of Proterozoic age [13, 51–53] and lies roughly in the north-western flank of doubly plunging syncline, and the road section is also dissected by thrust

faults [54]. The area is highly vulnerable to landslides due to adverse geo-structural paradigm. Many rocks and debris landslide have occurred in the region in the last few years [13, 55–57].

Meteorological and Seismological Conditions

Figure 3 shows the annual rainfall for the study area for a 31-year period from 1990 to 2021 for the study region. The annual average rainfall for a 30-year period is 1272.20 mm with the highest annual rainfall observed in the year 1995 (1870.19 mm) followed closely by 2010 (1860.46 mm). The lowest average rainfall is observed in the year 2009 with an average rainfall of 742.09 mm. Figure 3 also shows the monthly average rainfall for a 31-year period from January 1990 to December 2021. It can be seen from the graph that most of the rainfall occurs during the period from July to September comprising 80 to 85% of the annual rainfall.

The study area lies within the Lesser Himalayan sub-division and lies in an active seismic zone IV [59]. The area is bounded by the main boundary thrust (MBT) to the south and the Main Central Thrust (MCT) to the north [15]. Earthquake shocks of magnitude ranging from 5 to 6 on a Richter scale were recorded in 1809, 1816, 1966, 1967, 1968, 1969, 1979, 1986, 1991 and 1995 [60]. Khattri [61] has recorded 252 microearthquakes in Garhwal, which define a 140 km

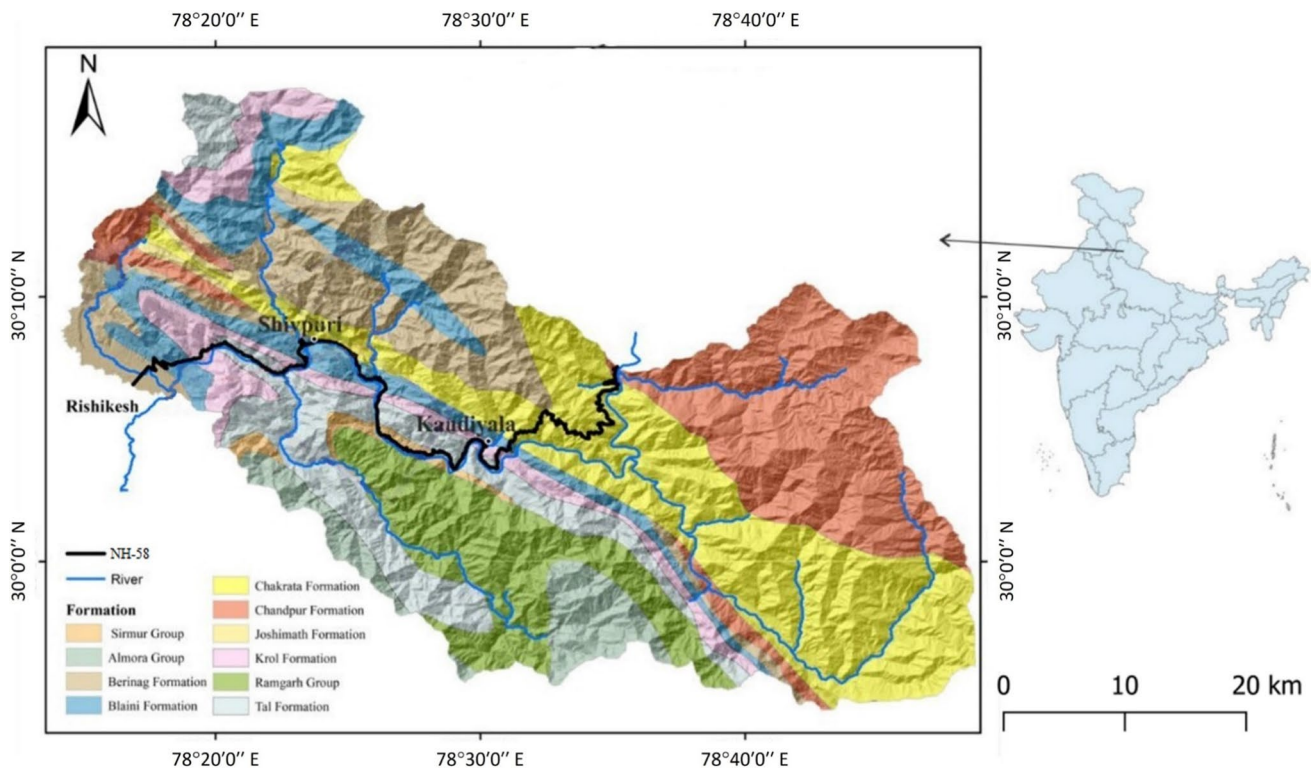


Fig. 2 Geological map of the study area (after Valdiya [58])

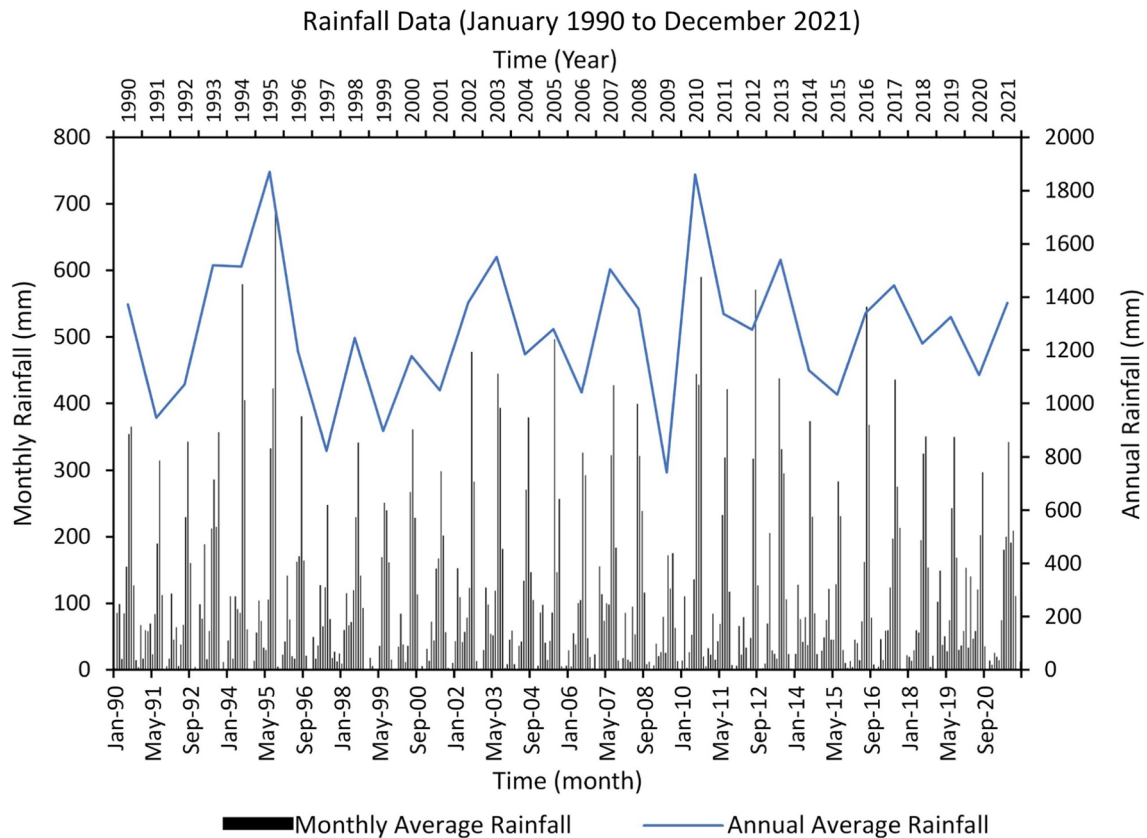


Fig. 3 Average rainfall received by Tehri Garhwal district during the period 1990 to 2021 (Source [63]:)

long belt trending NW–SE from Yamuna to Alaknanda Valley [62]. Most of the earthquakes in the Garhwal region occur close to the MCT. A total of 193 local earthquakes were estimated to have a depth of less than 10 km, while 32 earthquakes were in the range of 10 to 15 km [60].

Methodology

The methodology comprises of site visits, collection of field data and rock samples, laboratory tests and desk studies (Fig. 4).

Field Observations

Fifty steep cut rock slopes from different locations along the roads were selected in the field and detailed observations were made. Height of slope, slope angle, dip direction of slope, joint dip and dip direction were observed. Based on visual observations, the height of the slope was divided into two broad categories, i.e., safe and unsafe height. The safe height is determined based on the possibility of little to no failure. Up to the safe height, the slope can remain stable on its own and there is no presence of loose blocks

or seepage of water from the slope. The rocks are mostly fresh or slightly weathered. The unsafe height is the height from where if any failure, such as rock fall or mass flow, occurs, there will be high hazard due to the failure. They are designated in the field based on the presence of loose block, wedge formation, degree of weathering and the presence of water or dampening on the surface of the rock slopes. Both safe and unsafe height were recorded for each section. Mapping of the joints was done using scanline survey [64–67]. Scanline survey comprises of using a measuring tape (about 30 m) which is pinned with a masonry nail and wire to the rock face along its strike and maximum dip. Starting from the zero end, the scanline is scanned and the intersection distance for each discontinuity is recorded. Whenever a discontinuity trace is intersected, the properties of the discontinuity are recorded and tabulated. The properties include the intersection distance, orientation, semi-trace length, termination, roughness and curvature. Brunton compass (Fig. 6a) was used to measure the dip and dip direction of joint planes. Figure 5 shows a typical datasheet of scanline survey done in the field.

Observations were made on the roughness of the joints. The roughness profile of the joint was drawn using a 15 cm profilometer (Fig. 6b). The joint roughness coefficient

Fig. 4 Schematic diagram of workflow



(JRC) for each joint was obtained by comparing the roughness profile with the chart suggested by Barton and Choubey [68]. For each set of joints, several profiles were considered (Fig. 7) and the mean value of the JRC for the joint set was taken to represent the roughness of the joint.

A N-type rebound hammer was used to estimate the joint wall compressive strength (JCS) (Fig. 6c). At least 15 to 20

values of JCS were obtained at different portions of the slope and the mean value of the JCS is taken to represent the JCS.

Analysis of Joint Data

In addition to field observations, four important joint characteristics have been considered in this study to quantify the

SCANLINE SURVEY LOGGING FORM

Details of scanline:			Details of rock face:			Rock type		Quartzite					
Label	Slope 7		Location	30°4'22"N 78°29'42"E		Excavation method		Mechanical					
Trend	170° - 350°		Dip direction	100°		Condition of exposure							
Plunge	0°		Dip angle	75°-80°									
Trimming level			Non-overhanging / Overhanging			Comments							
Logged by			Height							20 m			
Date Logged			27-09-2019							Width			
Intersection distance d (m)	Dip Direction (°)	Dip Angle (°)	Semi-trace length l (m) above or left of scan	Semi-trace length l (m) below or right of scan	Termination l = 1, A = 2, O = 3		Roughness JRC 1-20	Curvature 1-5	Comments (Refer to table of abbreviations and codes)				
0.18	190	50	0.9	2.5	1	3	7	2					
0.25	220	45	6.0	1.3	2	3	11	2					
0.6	250	42	0.8	1.2	2	3	11	3					
1.5	190	50	1.5	1.0	1	2	9	1					
1.95	190	50	1.5	0.5	2	2	9	2					
2.03	190	50	5.0	0.4	2	1	9	2					
2.58	210	55	2.5	1.8	1	3	9	3					
2.7	215	55	1.0	0.1	2	2	13	5					
3.15	210	45	0.3	0.2	2	3	13	3					
3.4	205	45	9.5	0.3	3	2	15	3					

Fig. 5 A typical datasheet of scanline survey

instability of the cut slope, i.e., frequency, dip, dip direction and surface roughness.

Joint Frequency

Joint frequency governs the block size in a rock mass. It is well known that if joint frequency (Joints/meter) is high the rock mass will be weaker. Scanline survey data was used to get the joint frequency. The perpendicular distance between joints in a joint set is calculated by using the following equation [65]:

$$X_n = X_d \cos \alpha \quad (1)$$

where X_n is the perpendicular distance between two consecutive joints, X_d is the distance between two joints along the scanline. α is the acute angle between the scanline and the discontinuity normal and is obtained as

$$\alpha = \cos^{-1} \left| \cos (\alpha_n - \alpha_s) \cos \beta_n \cos \beta_s + \sin \beta_n \sin \beta_s \right| \quad (2)$$

α_n is the trend of the scanline, α_s is the trend of the normal of the discontinuity, β_n is the plunge of the scanline, and β_s is the plunge of the normal of the discontinuity.

Fig. 6 Instruments used for field observation. **a** Brunton compass **b** Barton comb profilometer **c** Schmidt Hammer N-type

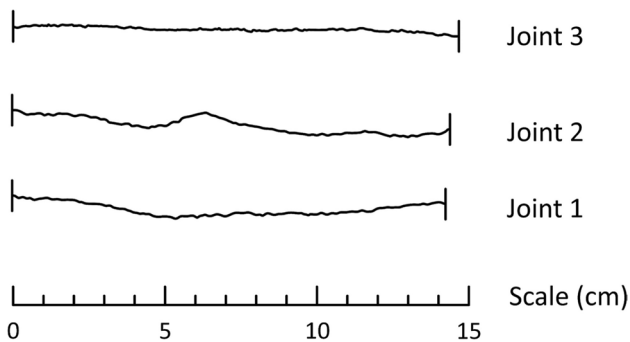
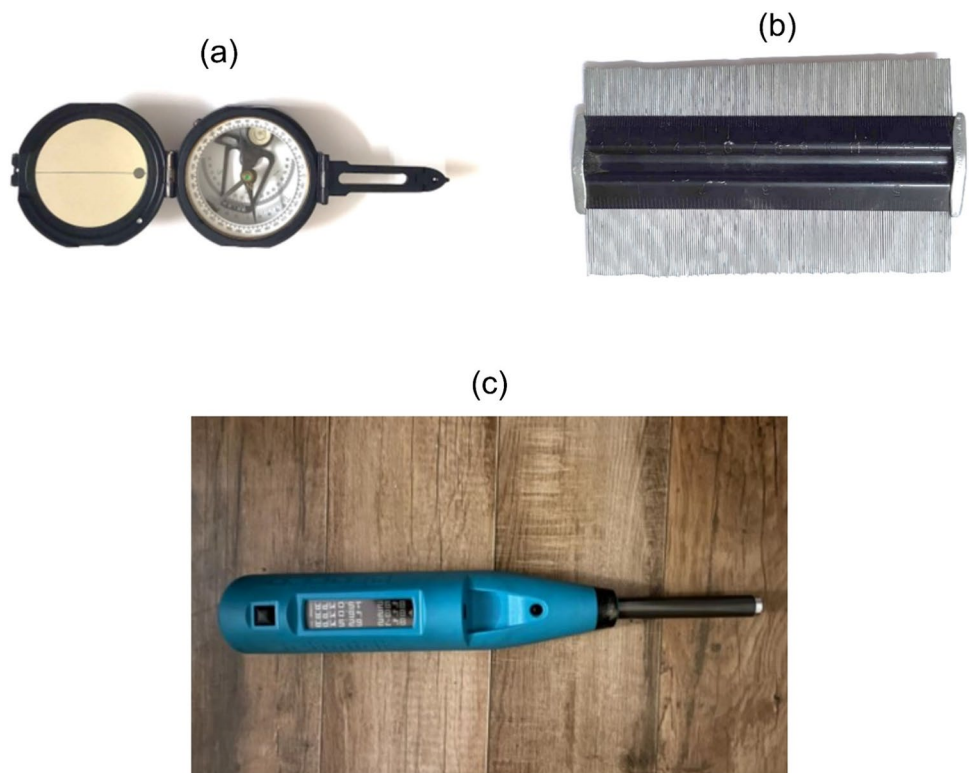


Fig. 7 Roughness profiles obtained from field study (Slope 1)

Spacing analyses were done on a scanline ranging from 10 to 25 m and the normal spacing of the joints was calculated based on the method provided by Priest [65]. Statistical analysis was done on the normal spacing of each joint set by considering the distribution reported in the literature [64, 66, 67, 69–73]. Anderson–Darling test [74] was done for each set, with a p value of 0.05. The distribution having the highest p value is taken for the distribution of the observed dataset (normal spacing of the joint). A histogram of the distribution is then drawn to represent the dataset (Fig. 8). It is observed that majority of the data follows either the exponential distribution or the Weibull distribution, with a few following the lognormal distribution (Fig. 8). The arithmetic mean of the spacing is determined which is used for

obtaining the spacing of the joints in the direction of loading as per Joint Factor concept. Some typical frequency distributions of the joint spacing observed are shown in Fig. 8.

Dip of Joint Plane

Dip of joint plane is a major factor that governs the likelihood of instability in a rock slope. In the present study, the effect of joint dip is quantified through a coefficient termed joint inclination parameter ‘ n ’ [8, 48, 75]. If a jointed specimen is tested with joint having variable inclination, the strength varies with inclination. The joint oriented at an angle of $(45^\circ + \phi/2)$ results in minimum strength [76]. The maximum strength of jointed specimen is obtained when loading is kept normal to joint plane. Arora [48] and Ramamurthy [49] correlated the influence of joint inclination with required frequency of horizontal joints that has an identical influence on the strength of jointed rocks. For example, it was found that an inclination of 40° was able to produce same effect as 26 horizontal joints in the rock [8]. By comparing the strength, the authors came out with the inclination parameter ‘ n ’ (Table 1).

Dip Direction of Joint Plane

Ideally, failure of rock slopes due to slip along the joint plane will be possible only when dip directions of slope and joint plane are same. As the angle between the dip

Fig. 8 Distribution of joint spacing data observed in the field **a** exponential **b** weibull **c** lognormal

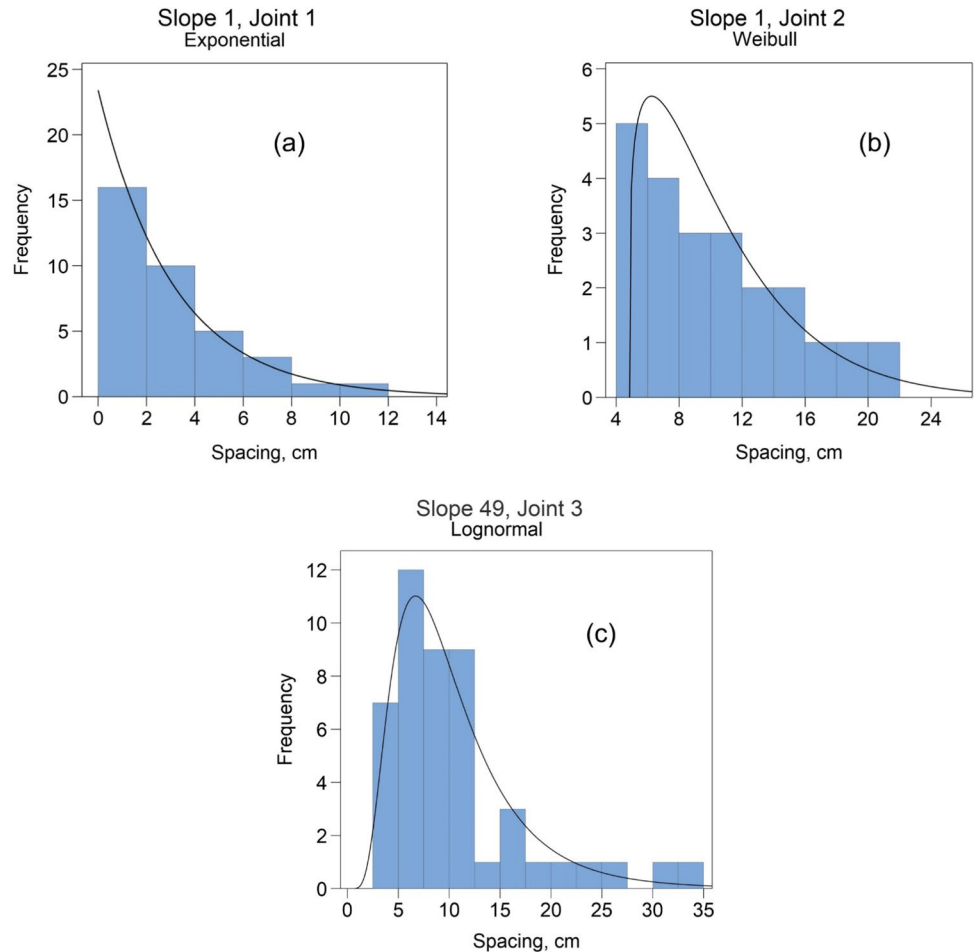


Table 1 Parameter for Joint Inclination (after Ramamurthy [49])

Orientation of joint θ ($^\circ$) ^a	0	10	20	30	40	50	60	70	80	90
Inclination Parameter, n	1.00	0.814	0.634	0.465	0.306	0.071	0.046	0.105	0.460	0.810

^a θ = angle between the normal to the joint plane and the direction of loading

direction of the slope and the joint plane increases, the effect of joint inclination tends to diminish. Both dip of joint plane and its dip direction jointly govern the instability. To account for impact of dip direction, the apparent dip of the joint plane in the dip direction of slope is considered in the present study. When dip directions are 90° apart, apparent dip will be 0°. If dip directions are more than 90° apart, the apparent dip of the joint plane is taken as 0°. The apparent dip is obtained as

$$\tan \psi = \tan \eta \cos \delta \tag{3}$$

where ψ is the apparent dip, η is the true dip of the joint, and δ is the difference between the dip direction of the slope face and the joint plane.

Surface Roughness of Joint Planes

The surface roughness of the joint surface is characterized through friction angle ϕ_j . Though the value of ϕ_j may be obtained by conducting direct shear tests along joint surface using field shear box [77], it will not be feasible in many situations. Alternatively, reliable estimates of joint friction angle can be made through Barton’s JRC-JCS joint shear strength model [68, 78]. The shear strength along a joint plane is represented by

$$\tau = \sigma_n \tan \left(\phi_r + \text{JRC} \log_{10} \left(\frac{\text{JCS}}{\sigma_n} \right) \right) \tag{4}$$

where τ is the shear strength, σ_n is the normal stress, JRC is the joint roughness coefficient, JCS is the joint wall compressive strength, and φ_r is the residual friction angle of the joint. The joint friction angle ϕ_j is given as

$$\phi_j = \phi_r + \text{JRC} \log_{10} \left(\frac{\text{JCS}}{\sigma_n} \right) \tag{5}$$

The angle ϕ_j is normal stress dependent and depends on the ratio JCS/σ_n . To simplify computations, the normal stress σ_n is taken equal to overburden pressure corresponding to the half of the height of the slope ($\gamma H/2$), where γ is unit weight of the rock mass in kN/m^3 .

Computation of Joint Factor

An index J_{f_slope} is introduced on lines similar to J_f concept. As compared to the Joint Factor, the J_{f_slope} has one more additional input parameter, i.e., angle between the dip direction of slope and joint plane. The J_{f_slope} is defined as

$$J_{f_slope} = \frac{J_n}{n_{corrected} \cdot r} \tag{6}$$

where J_n = number of joints per meter in vertical direction; $n_{corrected}$ is corrected value of inclination parameter ‘ n ’ where the correction is done based on the angle between the dip direction of slope and the joint plane, and ‘ r ’ is strength along the joint plane = $\tan(\phi_j)$.

The index J_{f_slope} quantifies the influence of joints on the rock slope. The J_{f_slope} is computed for all the joint sets observed in the field. The joint plane, which exhibits the maximum value of J_{f_slope} , is considered critical and governs the instability of the slope.

Results

The data generated through field studies was analyzed. Values of J_{f_slope} were computed for each section. As discussed in the previous section, the calculation of J_{f_slope} required height of slope, joint frequency, JRC of joint planes, dip of joint plane, angle between dip directions of joint plane and slope and JCS of the rock. Depending on the number of joints, there would be more than one J_{f_slope} for each section. The maximum J_{f_slope} was considered critical for each of the sections. A non-dimensional parameter normalized height was defined as:

$$\text{Normalized height} = \frac{\gamma H}{\sigma_c}$$

where γ is the unit weight of the rock in kN/m^3 ; H is the height of the slope in meter; and σ_c is the UCS of intact rock

in kPa. The normalized height is a non-dimensional number which links unit weight, height and UCS of intact rock with each other.

Normalized height was computed for observed safe as well as unsafe height. For each section, the normalized height for safe as well as unsafe height was plotted against J_{f_slope} . The J_{f_slope} was plotted on log scale, whereas normalized height was plotted on normal scale. The variation of normalized heights against J_{f_slope} is shown in Fig. 9. The plot shows two best fitting trend lines; the upper line represents safe height and the lower one unsafe height.

Discussions

The plots of J_{f_slope} versus normalized height ($\gamma H/\sigma_c$) indicate that the normalized heights decrease with increasing J_{f_slope} . This shows that there is a strong correlation of safe height and unsafe height of cut slope with joint attributes and intact rock strength. It is also observed that the trend lines for safe and unsafe heights run approximately parallel to each other. The plot can be divided into three distinct regions. The region below the safe height is designated as ‘low hazard’ region; the region between the safe height and unsafe height as ‘medium hazard’ and that above the unsafe height as ‘high hazard’ region. The boundaries of the regions are represented as:

$$\frac{\gamma H}{\sigma_c} = 0.01601 - 0.001864 \ln J_{f_slope} \tag{7}$$

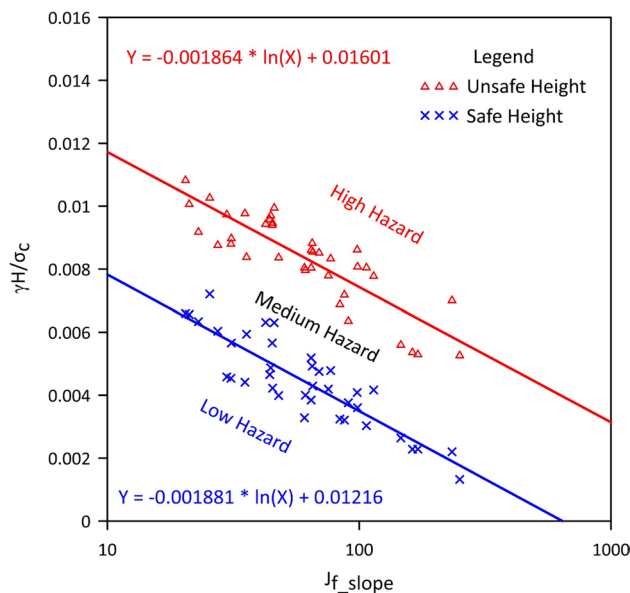


Fig. 9 Variation of normalized height of slope with J_{f_slope}

$$\frac{\gamma H}{\sigma_c} = 0.01216 - 0.001881 \ln J_{f_slope} \quad (8)$$

Equation (7) represents the boundary between ‘medium hazard’ and ‘high hazard’, while Eq. (8) represents the boundary between ‘medium hazard’ and ‘low hazard’.

Any slope represented by a point in these regions will represent the hazard related to that slope. To check the hazard of a given slope in the field, the normalized height and the J_{f_slope} may be obtained, and the point is plotted on Fig. 9 and the hazard due to the rock slope can be assessed. Figure 9 can also be used to quickly work out the upper limit of the safe height for a given joint attributes and rock properties. This quick assessment will be very useful when a quick decision about the height to which slopes should be cut is required especially during urgent situations.

Charts for Quick Assessment of Hazard due to Steep-Cut Rock Slope

In this section, charts are produced that can be used by field engineers for quick computations without going much into detail computations.

Chart for Quick Assessment of Joint Friction Angle

Joint friction angle is an important input parameter and is obtained based on JRC, JCS and assumed normal stress on the joint plane as discussed previously. A chart is produced for quick assessment of the friction angle. Figure 10 shows the chart between the ratio JCS/σ_n and the joint friction angle for various values of joint roughness coefficient. The graphs were produced using Eq. (5). The value of residual friction angle (φ_r) was chosen based on the results reported in Barton and Choubey [68]. Barton and Choubey has reported the residual friction angle of various rock types having varying JRC values, and it was reported to have values ranging from 24° to 32° . For simplicity in the calculation, the φ_r was taken equal to 28° . The JRC values were taken at a regular interval of 5, starting from 0 up to 20, and by linear interpolation, the value of the joint friction angle for a given value of JRC, JCS and σ_n can be easily obtained from the graph. Theoretically, very high value of φ_j approaching almost 90° may be possible. However, from practical point of view, a cap of about 65° is suggested for maximum value of φ_j in the field.

Multiple-Graph Technique for Assessment of Hazard Due to Steep-Cut Rock Slope in the Field

A multiple-graph technique for hazard assessment of the slopes in Garhwal Himalayas is proposed, which includes four subgraphs (Fig. 11).

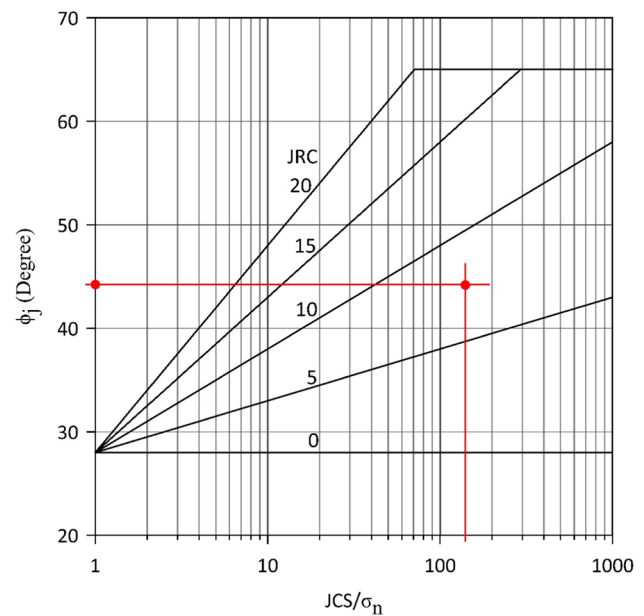


Fig. 10 Chart for predicting joint friction angle, φ_j

Graph I: Estimation of Apparent Dip of Joint Plane

While estimating the hazard due to steep-cut rock slopes, the first step is the estimation of the apparent dip of the joints. When the dip direction of the joint and the slope face are within 20° of each other, there is a high possibility of slip along the joint planes. The influence of the joint inclination decreases as the dip directions of the joint and the slope face move further away from each other, i.e., the difference of the dip direction of the slope face and the dip direction of the joint increases. When the dip directions are more than 90° apart, the apparent dip of the joint is taken as 0° . The apparent dip of a joint can be estimated using Eq. (3).

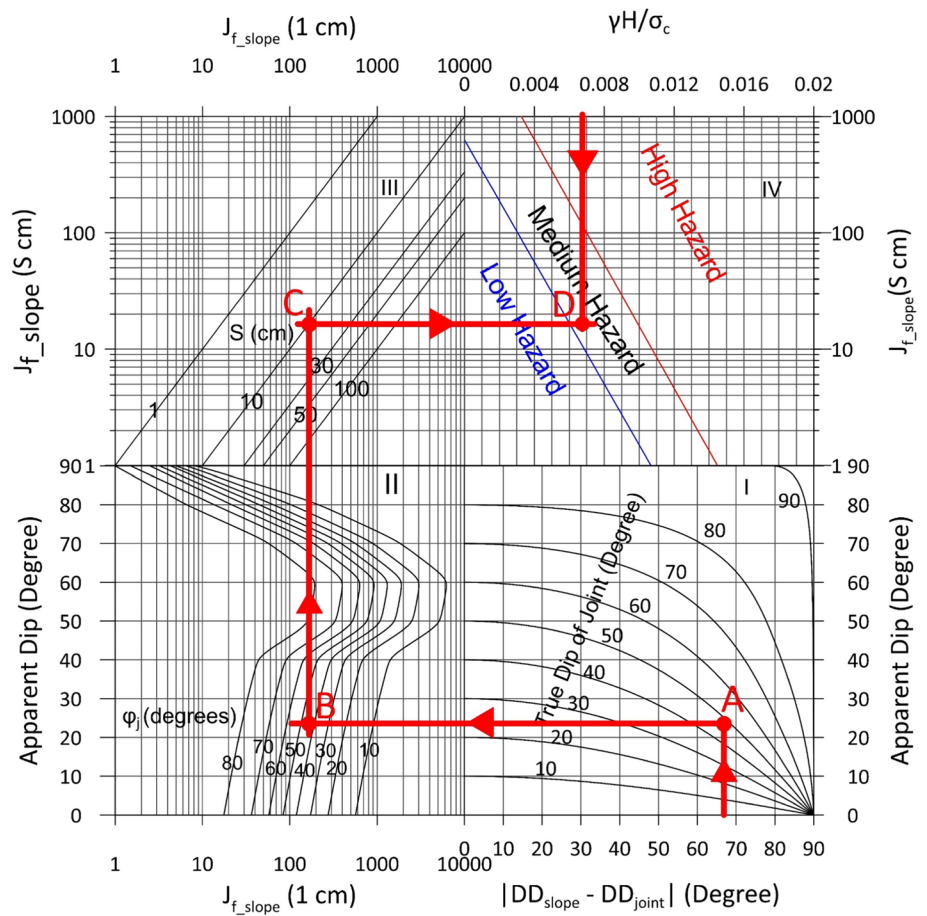
Graph I (Fig. 11) provides a set of curves which are drawn between the apparent dip and the difference between the dip direction of slope face and the joint for different values of true dip of joint. The graph is plotted on a normal scale. Knowing the difference between the dip direction of the slope face and the joint and the true dip of the joint, the apparent dip of the joint can be obtained from Graph I.

Graph II & III: Estimation of J_{f_slope}

The second step in the proposed method is the estimation of J_{f_slope} for each joint set in the slope.

A set of curves are given on a semi-log scale in Graph II (Fig. 11) between the apparent dip and the Joint Factor (J_{f_slope}) for a 1 cm joint spacing for different values of joint friction angles (φ_j). Knowing the value of the joint friction angle, the J_{f_slope} for a spacing of 1 cm can be determined from this graph.

Fig. 11 Multiple-graph technique proposed for preliminary assessment of hazard due to rock slopes



The actual value of J_{f_slope} in the field will be given by:

$$J_{f_slope} = \frac{J_{f_slope}(1 \text{ cm})}{S} \tag{9}$$

where J_{f_slope} (1 cm) is the Joint Factor for 1 cm spacing of the joints and S is the spacing of the joint in the field in centimeter.

A graph between the values of J_{f_slope} (1 cm) and J_{f_slope} (S cm) for different values of joint spacings is plotted on a log–log graph (Graph III). This graph can be used to obtain the value of J_{f_slope} for a given joint spacing, when the Joint Factor for a 1 cm spacing of the joints is known.

Graph IV: Estimation of Hazard on Steep-Cut Rock Slope

The final step in the proposed method is the estimation of the hazard due to steep-cut rock slope depending upon the J_{f_slope} obtained from graph III and the normalized height of the rock slope.

Graph IV presents the variation of the normalized height with the J_{f_slope} which is drawn from the data obtained from 50 rock slopes selected in the present study.

The step-by-step procedure to obtain the hazard due to steep-cut rock slope using the proposed multiple-graph technique is given below:

- (a) Collect field data: This includes the height of slope, dip and dip direction of slope face, dip and dip direction of the joint set, joint roughness coefficient, joint wall compressive strength, the normal spacing of joints and the unit weight of rock.
- (b) Obtain the joint friction angle from the chart provided in Fig. 10.
- (c) Using Graph I (Fig. 11) and based on the difference between the dip direction of the slope face and the dip direction of the joints, and the true dip of the joint, get point A on Graph I. An example is shown in Fig. 11. For a slope, $|DD_{slope} - DD_{joint}|$ is 67° and the dip of the joint is 48° . Point A in Graph I represents the apparent dip of the joint.
- (d) Using the value of ϕ_j obtained from step 2, move from point A to point B on Graph II.
- (e) Move to Graph III and obtain point C using the normal joint spacing S .
- (f) Calculate the normalized height ($\gamma H/\sigma_c$) for the rock slope and obtain point D on Graph IV, which will pro-

vide a rough estimate of the hazard due to the rock slope.

It should be noted that the proposed multiple-chart was made using the data collected from a specific site (in this case, National Highway-58), having a particular geology, lithology, meteorological conditions and seismicity. The applicability of the proposed multiple-chart is limited to sites having similar conditions. The applicability of the proposed multiple-chart on different geology and meteorological conditions can be taken up as a future studies. It is also reiterated that the charts should not be seen as a replacement of more rigorous stability analysis. The charts should only be used in the preliminary stages of design or when slope cutting is required at a faster rate, especially during the time of emergency.

Validation of Proposed Multiple-Graph Technique Through Case Studies

A demonstration of the proposed method is worked out in this section using the following set of data, which is obtained from the field:

Height of slope: 14 m.

Slope attitude: $49^\circ/217^\circ$

Normal spacing of the joint = 10.3 cm.

Joint attitude: $51.4^\circ/150^\circ$

Joint wall compressive strength (JCS) = 54.9 MPa.

Joint roughness coefficient: 8

Unit weight of rock: 27 kN/m^3 .

The solutions are shown in Figs. 10 and 11.

Solution

Step 1: Estimation of Joint Friction Angle

For the estimation of joint friction angle, the chart provided in Fig. 10 is used. From the data available, the following calculations are made:

$$\frac{\text{JCS}}{\sigma_n} = \frac{54.9 \times 1000}{27 \times 14} = 145.39$$

Using $(\text{JCS}/\sigma_n) = 145.4$, the value of joint friction angle for a $\text{JRC} = 8$ is obtained from the graph as 44°

Step 2: Assessment of Hazard Due to Steep-Cut Rock Slope Using Proposed Multiple Graph

From the given data, $|\text{DD}_{\text{slope}} - \text{DD}_{\text{joint}}| = 67^\circ$, the true dip of the joint = 51.4° . From Graph I, obtain point A which represents the apparent dip. From point A, move left and get point B in Graph II, corresponding to the value of ϕ_j . From point B, move vertically upward and get point C corresponding to the joint spacing.

From point C, move horizontally toward the right side to obtain point D. The region in which point D lies indicates the hazard due to the rock slope.

Similarly, the proposed chart is used for five different slopes (labeled as S-1 to S-5) having varying degrees of stability. Slopes 1, 2 and 5 are partially stable slopes. Slope 3 is a failed slope, where the joint sets are closely spaced, and the most critical joint set runs in the same direction as the slope face. In the case of slope 4, the joint sets are favorably oriented in such a way that they can remain stable on their own. Table 2 shows the data obtained for hazard estimation for each site. Figure 12 shows the slopes used for validation of the proposed chart. Figure 13 shows the different points corresponding to the hazard due to the rock slope. By comparing the results obtained from the chart and the observations made in the field, the observation made from the proposed chart provides a reliable estimate of the hazard due to the steep-cut rock slopes.

Table 2 Parameters used for validation of proposed chart

Site no	Slope face		Joint plane		DD _s —DD _j	Joint spacing, cm	$\phi_j(^{\circ})$	$J_{f,\text{slope}}$	$\frac{\gamma H}{\sigma_c}$
	Dip	Dip direction	Dip	Dip direction					
S-1	49	217	51.4	150	67	10.3	44.05	16.42	0.0069
S-2	55	273	57.5	299	26	10.52	49.42	102.93	0.0089
S-3	48	200	45	195	5	7.25	36.53	115.09	0.0170
S-4	43	295	51	67	228	18.52	60	3.12	0.0046
S-5	52	290	52	280	10	9.45	53	94.60	0.0069

Fig. 12 Photograph of site used for validation of proposed chart
 a S-1 b S-2 c S-3 d S-4 e S-5

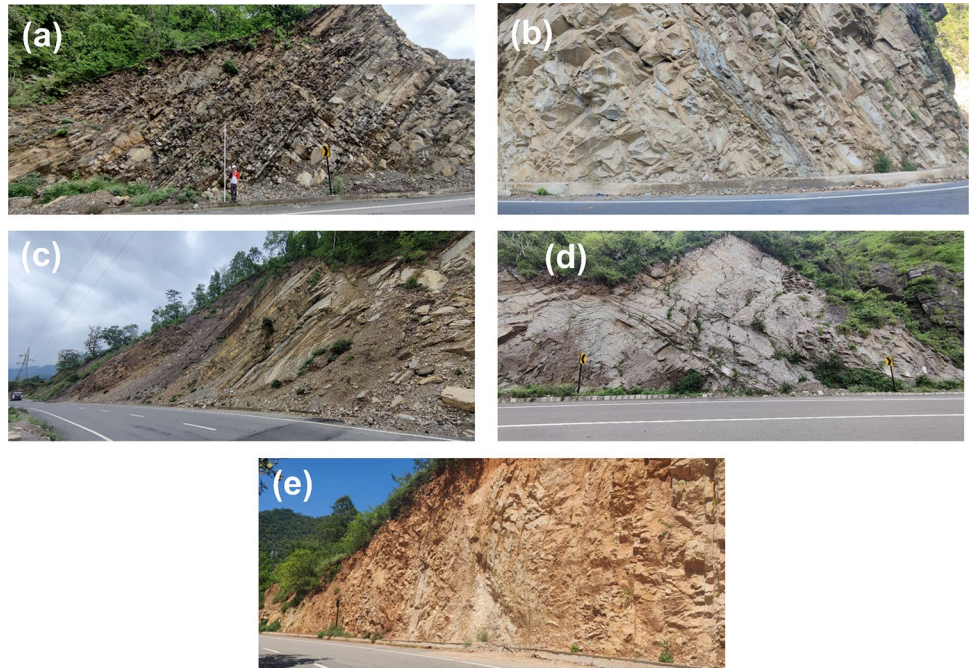
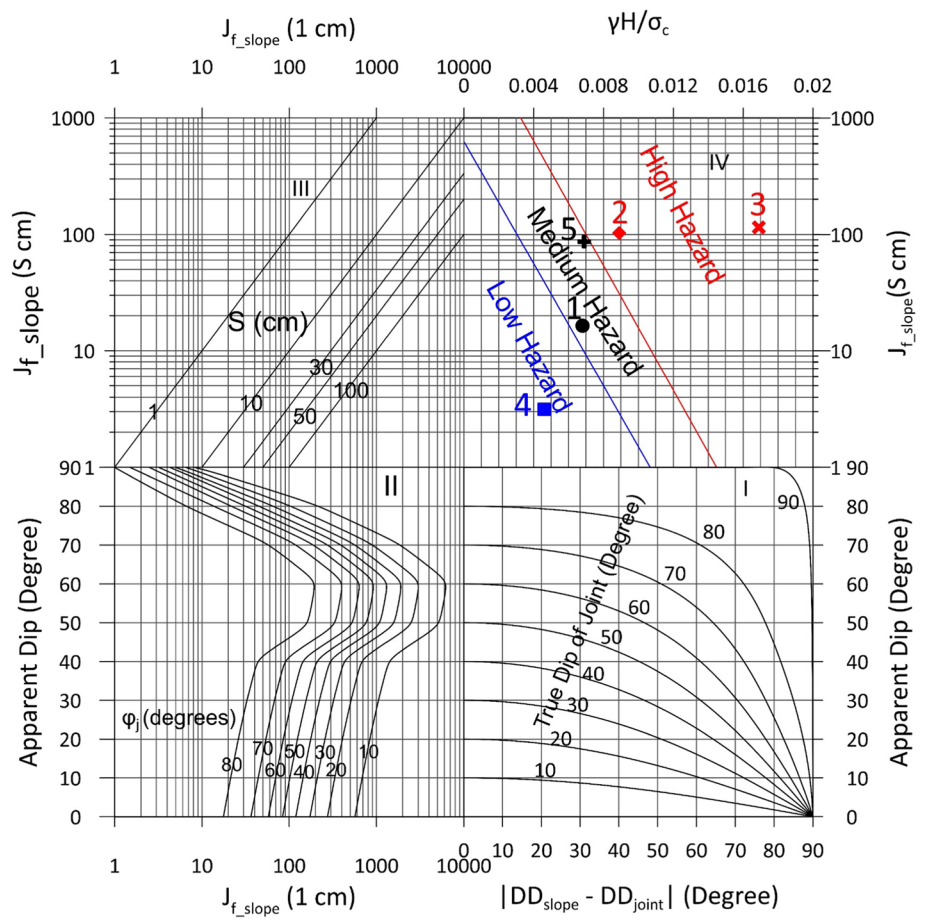


Fig. 13 Result of hazard assessment on rock slope using data obtained from field



Concluding Remarks

A simple approach is presented for estimating the approximate value of the safe height and the hazard due to steep-cut rock slopes in Garhwal region. The approach has been developed based on extensive field study followed by laboratory and desk study. Fifty rock slopes showing signs of instability were selected along the National Highway—58 and studied in detail.

An index J_{f_slope} has been developed based on Joint Factor concept for jointed rock slopes. The index incorporates the effect of joint attributes (dip, dip direction, spacing and roughness) and slope geometry (dip and dip direction of slope face). The height of slope is normalized through the unit weight of rock and strength of the intact rock. A strong correlation is observed between the safe height of the slope and the index J_{f_slope} . Using this correlation, conditions of low, medium and high hazard due to rock slopes are defined. Based on simple, easy-to-obtain input from field, one can quickly assess the hazard due to an existing or proposed cut slope. To help field engineers, multigraph technique is suggested for quick assessment of the hazard due to rock slope and safe height of slope for the region.

Acknowledgements A part of financial support for this study was received from National Disaster Management Authority (NDMA), Ministry of Home Affairs Government of India, New Delhi (Project No. NDM-1503-CED/19-20). The authors thankfully acknowledge the support received from NDMA.

Author Contributions LH and MS were involved in conceptualization. LH, MS, and SPP helped in methodology. LH and JS contributed to formal analysis and investigation. LH was involved in writing—original draft preparation. MS helped in writing—review and editing. MS contributed to funding acquisition. MS and SPP helped in resources. MS and SPP were involved in supervision.

Funding A part of the financial support for the present study has been received from National Disaster Management Authority (NDMA), Ministry of Home Affairs, Government of India, New Delhi.

Declarations

Conflict of interest The authors declare that they have no conflict of interest.

References

- Bieniawski ZT (1973) Engineering classification of jointed rock masses. In: Transaction of the South African Institution of Civil Engineers, pp 335–344
- Romana M (1985) New adjustment ratings for application of Bieniawski classification to slopes. In: International symposium on the role of rock mechanics in excavations for mining and civil works. International Society of Rock Mechanics, Zacatecas, pp 49–53
- Marinos V, Marinos P, Hoek E (2005) The geological strength index: applications and limitations. *Bull Eng Geol Env* 64:55–65. <https://doi.org/10.1007/s10064-004-0270-5>
- Morelli GL (2017) Alternative quantification of the geological strength index chart for jointed rocks. *Geotech Geol Eng* 35:2803–2816. <https://doi.org/10.1007/s10706-017-0279-8>
- Marinos V, Marinos P, Hoek E (2010) Geological strength index (GSI). A characterization tool for assessing engineering properties for rock masses. In: Underground works under special conditions. <https://doi.org/10.1201/noe0415450287.ch2>
- Barton N, Lien R, Lunde J (1974) Engineering classification of rock masses for the design of tunnel support. *Rock Mech* 6:189–236. <https://doi.org/10.1007/BF01239496>
- Ramamurthy T (1985) Stability of rock mass. *Indian Geotech J* 8:1–74
- Ramamurthy T, Arora VK (1994) Strength predictions for jointed rocks in confined and unconfined states. *Int J Rock Mech Min Sci* 31:9–22. [https://doi.org/10.1016/0148-9062\(94\)92311-6](https://doi.org/10.1016/0148-9062(94)92311-6)
- Singh M, Rao KS, Ramamurthy T (2002) Strength and deformational behaviour of a jointed rock mass. *Rock Mech Rock Eng* 35:45–64. <https://doi.org/10.1007/s006030200008>
- Kanungo DP, Pain A, Sharma S (2013) Finite element modeling approach to assess the stability of debris and rock slopes: a case study from the Indian Himalayas. *Nat Hazards* 69:1–24. <https://doi.org/10.1007/s11069-013-0680-4>
- Ray A, Kumar RESC, Bharati AK et al (2020) Hazard chart for identification of potential landslide due to the presence of residual soil in the Himalayas. *Indian Geotech J* 50:604–619. <https://doi.org/10.1007/s40098-019-00401-6>
- Siddique T, Pradhan SP, Vishal V et al (2017) Stability assessment of Himalayan road cut slopes along National Highway 58. *India Environ Earth Sci* 76:759. <https://doi.org/10.1007/s12665-017-7091-x>
- Siddique T, Pradhan SP, Vishal V, Singh TN (2020) Applicability of Q-slope method in the Himalayan road cut rock slopes and its comparison with CSMR. *Rock Mech Rock Eng* 53:4509–4522. <https://doi.org/10.1007/s00603-020-02176-2>
- NDMA (2021) Generation of meso-level 1:10,000 scale user friendly landslide hazard zonation (LHZ) maps and landslide inventory for Tapovan—Vyasi corridor of Haridwar—Badrinath National Highway (NH-58), Uttarakhand
- Nath RR, Das N, Satyam DN (2021) Impact of main boundary thrust (MBT) on landslide susceptibility in Garhwal Himalaya: a case study. *Indian Geotech J* 51:746–756. <https://doi.org/10.1007/s40098-021-00522-x>
- Kumar S, Pandey HK (2021) Slope stability analysis based on rock mass rating, geological strength index and kinematic analysis in Vindhyan rock formation. *J Geol Soc India* 97:145–150. <https://doi.org/10.1007/s12594-021-1645-y>
- Romana M (1993) A geomechanical classification for slopes: slope mass rating. In: Rock testing and site characterization. Elsevier, pp 575–600
- Tomás R, Delgado J, Serón JB (2007) Modification of slope mass rating (SMR) by continuous functions. *Int J Rock Mech Min Sci* 44:1062–1069. <https://doi.org/10.1016/j.ijrmms.2007.02.004>
- Riquelme AJ, Tomás R, Abellán A (2016) Characterization of rock slopes through slope mass rating using 3D point clouds. *Int J Rock Mech Min Sci* 84:165–176. <https://doi.org/10.1016/j.ijrmms.2015.12.008>
- Romana M, Tomás R, Serón JB (2015) Slope mass rating (SMR) geomechanics classification: thirty years review. IS. In: ISRM congress 2015 proceedings—international symposium on rock mechanics, Quebec, Canada, p 10
- Siddique T, Masroor Alam M, Mondal MEA, Vishal V (2015) Slope mass rating and kinematic analysis of slopes along the national highway-58 near Jonk, Rishikesh, India. *J Rock Mech*

- Geotech Eng 7:600–606. <https://doi.org/10.1016/j.jrmge.2015.06.007>
22. Bar N, Barton N (2018) Q-slope: an empirical rock slope engineering approach in Australia. *Aust Geomech J* 53:73–86
 23. Bar N, Barton N (2017) The Q-slope method for rock slope engineering. *Rock Mech Rock Eng* 50:3307–3322. <https://doi.org/10.1007/s00603-017-1305-0>
 24. Bar N, McQuillan A (2021) Q-slope and SSAM applied to excavated coal mine slopes. *MethodsX* 8:101191. <https://doi.org/10.1016/j.mex.2020.101191>
 25. Bar N, Barton N (2018) Rock slope design using q-slope and geophysical survey data. *Period Polytech Civ Eng* 62:893–900. <https://doi.org/10.3311/PPci.12287>
 26. Bar N, Barton NR (2016) Empirical slope design for hard and soft rocks using Q-slope. In: 50th US Rock mechanics/geomechanics symposium 2016, vol 2, pp1301–1308
 27. De Paula MS, Maion AV, Campanha GAC et al (2020) Q-slope and rhrs for the evaluation of highway rock slopes—Serrado Mar, Brazil. *Rock mechanics for natural resources and infrastructure development-proceedings of the 14th international congress on rock mechanics and rock engineering. ISRM 2019*, pp 3490–3497
 28. Barton N, Bar N (2015) Introducing the Q-slope method and its intended use within civil and mining engineering projects. *ISRM Region Symp EUROCK 2015*:157–162
 29. Azarafza M, Nanehkaran YA, Rajabion L et al (2020) Application of the modified Q-slope classification system for sedimentary rock slope stability assessment in Iran. *Eng Geol* 264:105349. <https://doi.org/10.1016/j.enggeo.2019.105349>
 30. Akhtar W, Siddique T, Haris PM et al (2023) An integrated geotechnical study using Q-slope method and factor of safety appraisal along NH-5 from Solan to Shimla, India. *J Earth Syst Sci*. <https://doi.org/10.1007/s12040-023-02104-2>
 31. Vishal V, Siddique T, Purohit R et al (2017) Hazard assessment in rockfall-prone Himalayan slopes along National Highway-58, India: rating and simulation. *Nat Hazards* 85:487–503. <https://doi.org/10.1007/s11069-016-2563-y>
 32. Lenka SK, Panda SD, Kanungo DP, Anbalagan R (2017) Slope mass assessment of road cut rock slopes along Karnprayag to Narainbagarh highway in Garhwal Himalayas, India. In: Mikoš M, Vilímek V, Yin Y, Sassa K (eds) *Advancing culture of living with landslides*. Springer, Cham, pp 407–413
 33. Kundu J, Sarkar K, Tripathy A, Singh TN (2017) Qualitative stability assessment of cut slopes along the National Highway-05 around Jhakri area, Himachal Pradesh, India. *J Earth Syst Sci*. <https://doi.org/10.1007/s12040-017-0893-0>
 34. Sarkar S, Kanungo DP, Kumar S (2012) Rock mass classification and slope stability assessment of road cut slopes in Garhwal Himalaya, India. *Geotech Geol Eng* 30:827–840. <https://doi.org/10.1007/s10706-012-9501-x>
 35. Ansari MK, Ahmad M, Singh R (2013) Rockfall hazard rating system for Indian Rockmass
 36. Ansari MK, Ahmad M, Singh R, Singh TN (2016) Rockfall hazard rating system along SH-72: a case study of Poladpur-Mahabaleshwar road (Western India), Maharashtra, India. *Geomat Nat Haz Risk* 7:649–666. <https://doi.org/10.1080/19475705.2014.1003416>
 37. Verma AK, Sardana S, Sharma P et al (2019) Investigation of rockfall-prone road cut slope near Lengpui Airport, Mizoram, India. *J Rock Mech Geotech Eng* 11:146–158. <https://doi.org/10.1016/j.jrmge.2018.07.007>
 38. Gupta AK, Mukherjee MK (2022) Evaluating Road-cut slope stability using newly proposed stability charts and rock microstructure: an example from Dharasu-Uttarkashi Roadway, Lesser Himalayas, India. *Rock Mech Rock Eng* 55:3959–3995. <https://doi.org/10.1007/s00603-022-02846-3>
 39. Komadja GC, Pradhan SP, Roul AR et al (2020) Assessment of stability of a Himalayan road cut slope with varying degrees of weathering: a finite-element-model-based approach. *Heliyon*. <https://doi.org/10.1016/j.heliyon.2020.e05297>
 40. Pradhan SP, Vishal V, Singh TN (2018) Finite element modelling of landslide prone slopes around Rudraprayag and Agastyamuni in Uttarakhand Himalayan terrain. *Nat Hazards* 94:181–200. <https://doi.org/10.1007/s11069-018-3381-1>
 41. Ghosh S, Kumar A, Bora A (2014) Analyzing the stability of a failing rock slope for suggesting suitable mitigation measure: a case study from the Theng rockslide, Sikkim Himalayas, India. *Bull Eng Geol Env* 73:931–945. <https://doi.org/10.1007/s10064-014-0586-8>
 42. Pradhan SP, Siddique T (2020) Stability assessment of landslide-prone road cut rock slopes in Himalayan terrain: a finite element method based approach. *J Rock Mech Geotech Eng* 12:59–73. <https://doi.org/10.1016/j.jrmge.2018.12.018>
 43. Zheng J, Zhao Y, Lü Q et al (2016) A discussion on the adjustment parameters of the slope mass rating (SMR) system for rock slopes. *Eng Geol* 206:42–49. <https://doi.org/10.1016/j.enggeo.2016.03.007>
 44. Pinheiro M, Sanches S, Miranda T, Neves A, Tinoco J. AF and AGC SQI—a quality assessment index for rock slopes
 45. Pierson LA (1991) Rockfall hazard rating system
 46. Budetta P (2004) Assessment of rockfall risk along roads. *Nat Hazard* 4:71–81. <https://doi.org/10.5194/nhess-4-71-2004>
 47. Bar N, Barton NR, Ryan CA (2016) Application of the Q-slope method to highly weathered and saprolitic rocks in Far North Queensland. *ISRM Int Symp EUROCK 2016*:585–590
 48. Arora VK (1987) Strength and deformational behaviour of jointed rocks. PhD Thesis, IIT Delhi
 49. Ramamurthy T (1993) Strength and modulus response of anisotropic rocks. *Comprehensive rock engineering*. Pergamon Press, Oxford, pp 313–329
 50. Singh M (1997) Engineering behavior of jointed model materials. PhD Thesis, Indian Institute of Technology, Delhi
 51. Jiang G, Christie-Blick N, Kaufman AJ et al (2003) Carbonate platform growth and cyclicity at a terminal Proterozoic passive margin, Infra Krol Formation and Krol Group, Lesser Himalaya, India. *Sedimentology* 50:921–952. <https://doi.org/10.1046/j.1365-3091.2003.00589.x>
 52. Tiwari M, Parcha SK, Shukla R, Joshi H (2013) Ichnology of the Early Cambrian Tal Group, Mussoorie Syncline, Lesser Himalaya, India. *J Earth Syst Sci* 122:1467–1475. <https://doi.org/10.1007/s12040-013-0360-5>
 53. Singh J, Pradhan SP, Singh M, Hruaikima L (2022) Control of structural damage on the rock mass characteristics and its influence on the rock slope stability along National Highway-07, Garhwal Himalaya, India: an ensemble of discrete fracture network (DFN) and distinct element method (DEM). *Bull Eng Geol Env* 81:96. <https://doi.org/10.1007/s10064-022-02575-5>
 54. Kumar G, Dhaundiyal JN (1979) Stratigraphy and structure of Garhwal Synform, Garhwal and Tehri Garhwal districts, Uttar Pradesh; a reappraisal. *Himalayan Geol* 9:18–41
 55. Valdiya KS (1988) Tectonics and evolution of the central sector of the Himalaya. *Philos Trans Roy Soc Lond Ser A Math Phys Sci* 326:151–175. <https://doi.org/10.1098/rsta.1988.0083>
 56. Sangeeta S, Maheshwari BK (2022) Spatial predictive modelling of rainfall- and earthquake-induced landslide susceptibility in the Himalaya region of Uttarakhand, India. *Environ Earth Sci*. <https://doi.org/10.1007/s12665-022-10352-6>
 57. Sati SP, Gahalaut VK (2013) The fury of the floods in the north-west Himalayan region: the Kedarnath tragedy. *Geomat Nat Haz Risk* 4:193–201. <https://doi.org/10.1080/19475705.2013.827135>
 58. Valdiya KS (1984) Evolution of the Himalaya. *Tectonophysics* 105:229–248. [https://doi.org/10.1016/0040-1951\(84\)90205-1](https://doi.org/10.1016/0040-1951(84)90205-1)

59. BIS (2016) IS: 1893 (Part-1) Indian standard, criteria for earthquake resistant design of structures: general provisions and buildings, New Delhi
60. Shandilya AK, Shandilya A (2016) Studies on the seismicity in Garhwal Himalaya, India. In: Raju NJ (ed) Geostatistical and geospatial approaches for the characterization of natural resources in the environment. Springer, Cham, pp 503–512
61. Khattri KN (1992) Seismic hazard in Indian region. *Curr Sci* 62:109–116
62. Gaur VK, Chander R, Sarkar I et al (1985) Seismicity and the state of stress from investigations of local earthquakes in the Kumaon Himalaya. *Tectonophysics* 118:243–251. [https://doi.org/10.1016/0040-1951\(85\)90123-4](https://doi.org/10.1016/0040-1951(85)90123-4)
63. India-WRIS. <https://indiawris.gov.in/wris/>. Accessed 30 Oct 2022
64. Priest SD, Hudson JA (1981) Estimation of discontinuity spacing and trace length using scanline surveys. *Int J Rock Mech Min Sci* 18:183–197. [https://doi.org/10.1016/0148-9062\(81\)90973-6](https://doi.org/10.1016/0148-9062(81)90973-6)
65. Priest SD (1993) Discontinuity analysis for rock engineering. Springer, Dordrecht
66. Hudson JA, Priest SD (1983) Discontinuity frequency in rock masses. *Int J Rock Mech Min Sci* 20:73–89. [https://doi.org/10.1016/0148-9062\(83\)90329-7](https://doi.org/10.1016/0148-9062(83)90329-7)
67. Priest SD, Hudson JA (1976) Discontinuity spacings in rock. *Int J Rock Mech Min Sci*. [https://doi.org/10.1016/0148-9062\(76\)90818-4](https://doi.org/10.1016/0148-9062(76)90818-4)
68. Barton N, Choubey V (1977) The shear strength of rock joints in theory and practice. *Rock Mech* 10:1–54. <https://doi.org/10.1007/BF01261801>
69. Becker A, Gross MR (1996) Mechanism for joint saturation in mechanically layered rocks: an example from southern Israel
70. Pascal C, Angelier J, Hancock PL (1997) Distribution of joints: probabilistic modelling and case study near Cardiff (Wales, U.K.)
71. Wong LNY, Lai VSK, Tam TPY (2018) Joint spacing distribution of granites in Hong Kong. *Eng Geol* 245:120–129. <https://doi.org/10.1016/j.enggeo.2018.08.009>
72. Castaing C, Halawani MA, Gervais F et al (1996) Scaling relationships in intraplate fracture systems related to Red Sea rifting. *Tectonophysics* 261:291–314. [https://doi.org/10.1016/0040-1951\(95\)00177-8](https://doi.org/10.1016/0040-1951(95)00177-8)
73. Ji S, Saruwatari K (1998) A revised model for the relationship between joint spacing and layer thickness. *J Struct Geol* 20:1495–1508. [https://doi.org/10.1016/S0191-8141\(98\)00042-X](https://doi.org/10.1016/S0191-8141(98)00042-X)
74. Stephens MA (1974) EDF statistics for goodness of fit and some comparisons. *J Am Stat Assoc* 69:730. <https://doi.org/10.2307/2286009>
75. Yaji RK (1984) Shear strength and deformation response of jointed rocks. PhD Thesis, IIT Delhi
76. Jaeger JC, Cook NGW (1969) Fundamentals of rock mechanics. Methuen
77. Franklin JA, Kanji MA, Herget G et al (1974) Suggested method for determining shear strength. In: Commission on standardization of laboratory and field tests. International Society for Rock Mechanics, pp 131–140
78. Barton N (1976) The shear strength of rock and rock joints. *Int J Rock Mech Min Sci Geomech Abstr* 13:255–279. [https://doi.org/10.1016/0148-9062\(76\)90003-6](https://doi.org/10.1016/0148-9062(76)90003-6)

Publisher's Note Springer Nature remains neutral with regard to jurisdictional claims in published maps and institutional affiliations.

Springer Nature or its licensor (e.g. a society or other partner) holds exclusive rights to this article under a publishing agreement with the author(s) or other rightsholder(s); author self-archiving of the accepted manuscript version of this article is solely governed by the terms of such publishing agreement and applicable law.